

Linkage between ATP Consumption and Mechanical Unfolding during the Protein Processing Reactions of an AAA⁺ Degradation Machine

Jon A. Kenniston,¹ Tania A. Baker,^{1,2}
Julio M. Fernandez,³ and Robert T. Sauer^{1,*}

¹Department of Biology

²Howard Hughes Medical Institute
Massachusetts Institute of Technology
Cambridge, Massachusetts 02139

³Department of Biological Sciences
Columbia University
New York, New York 10027

Summary

Proteolytic machines powered by ATP hydrolysis bind proteins with specific peptide tags, denature these substrates, and translocate them into a sequestered compartment for degradation. To determine how ATP is used during individual reaction steps, we assayed ClpXP degradation of *ssrA*-tagged titin variants with different stabilities in native and denatured forms. The rate of ATP turnover was 4-fold slower during denaturation than translocation. Importantly, this reduced turnover rate was constant during denaturation of native variants with different stabilities, but total ATP consumption increased with substrate stability, suggesting an iterative application of a uniform, mechanical unfolding force. Destabilization of substrate structure near the degradation tag accelerated degradation and dramatically reduced ATP consumption, revealing an important role for local protein stability in resisting denaturation. The ability to denature more stable proteins simply by using more ATP endows ClpX with a robust unfolding activity required for its biological roles in degradation and complex disassembly.

Introduction

Intracellular AAA⁺ ATPases function in degrading proteins, transporting cargo along microtubules, fusing vesicles, driving protein secretion, dismantling hyperstable oligomeric structures, resuspending protein aggregates, and unwinding double-stranded nucleic acids (Neuwald et al., 1999; Vale, 2000; Langer, 2000; Ogura and Wilkinson, 2001). All cells contain compartmentalized AAA⁺ proteases in which one or more ATPases act to bind substrates, denature these molecules, and translocate the denatured polypeptide into a protected proteolytic chamber for degradation (Langer, 2000). In eukaryotes, the proteasome is a prominent AAA⁺ degradation machine. In bacteria, ATPases of the Clp/HSP100 family power energy-dependent degradation for the ClpXP, ClpAP, Lon, HslUV, and FtsH proteases.

Many questions about the mechanisms employed by this ubiquitous family of AAA⁺ proteases remain unresolved. Does protein denaturation occur by mechanical application of force? How is resistance to degradation related to protein stability? Does ATP consumption vary

with native protein stability? How is ATP utilized during individual steps in the degradation reaction? Moreover, despite the sequence and architectural similarities between different AAA⁺ enzymes, recent studies highlight what appear to be significant differences. For instance, unfolding of a GFP substrate appears to be kinetically irrelevant for degradation by the archaeobacterial PAN/20S protease (Benaroudj et al., 2003), an impediment to degradation by ClpXP (Kim et al., 2000), and a step that the FtsH protease is unable to perform (Herman et al., 2003).

Our attention has been focused on *E. coli* ClpXP, a well-characterized AAA⁺ machine that destroys proteins bearing specific degradation signals (Gottesman et al., 1998; Gonciarz-Swiatek et al., 1999; Flynn et al., 2003). For example, the 11-residue *ssrA* degradation tag, which is added to the C terminus of proteins unable to complete normal translation (Keiler et al., 1996), targets any protein for ClpXP degradation. Figure 1 summarizes our current view of the ClpXP degradation cycle. The active-site residues of the ClpP peptidase are located in an internal chamber accessible through restricted entry portals (Wang et al., 1997). ClpX, a hexameric AAA⁺ ATPase, catalyzes both the ATP-dependent denaturation of protein substrates and their energy-dependent translocation into ClpP for degradation (Kim et al., 2000; Singh et al., 2000; Ortega et al., 2002). Because substrate degradation and product release by ClpP are fast (Thompson and Maurizi, 1994; Thompson et al., 1994), the binding, denaturation, and translocation steps should be the principal determinants of the rate of ClpXP protein degradation.

How does the stability of proteins affect their rate of degradation by ClpXP? Experiments using *ssrA*-tagged variants of different proteins show that ClpX-mediated denaturation is an active process and modulating stability through mutations or ligand binding affects degradation in some but not all cases (Kim et al., 2000; Burton et al., 2001a; Lee et al., 2001). To explain this variability, Matouschek and colleagues proposed that the local stability of structure adjacent to the degradation tag rather than global stability determines the rate of protein denaturation and subsequent degradation (Lee et al., 2001; Matouschek, 2003). This model makes sense if ClpXP initiates unfolding by “pulling” on the degradation tag and therefore must unravel the adjacent structure first. However, changes in the structural properties of substrates might also influence ClpXP degradation in other ways, and thus determining the effects of substrate alterations on the binding, denaturation, and translocation steps of the overall reaction is important for understanding the mechanism of this ATP-dependent protease.

To deconvolute the steps and energy requirements for ClpXP degradation, we sought a model substrate and variants with four features: (1) known or determinable native stabilities; (2) the existence of soluble denatured variants; (3) well-characterized stability to mechanical unfolding by atomic-force microscopy (AFM); and (4) the availability of variants displaying a range of local protein stabilities at the C terminus, the site of *ssrA*

*Correspondence: bobsauer@mit.edu

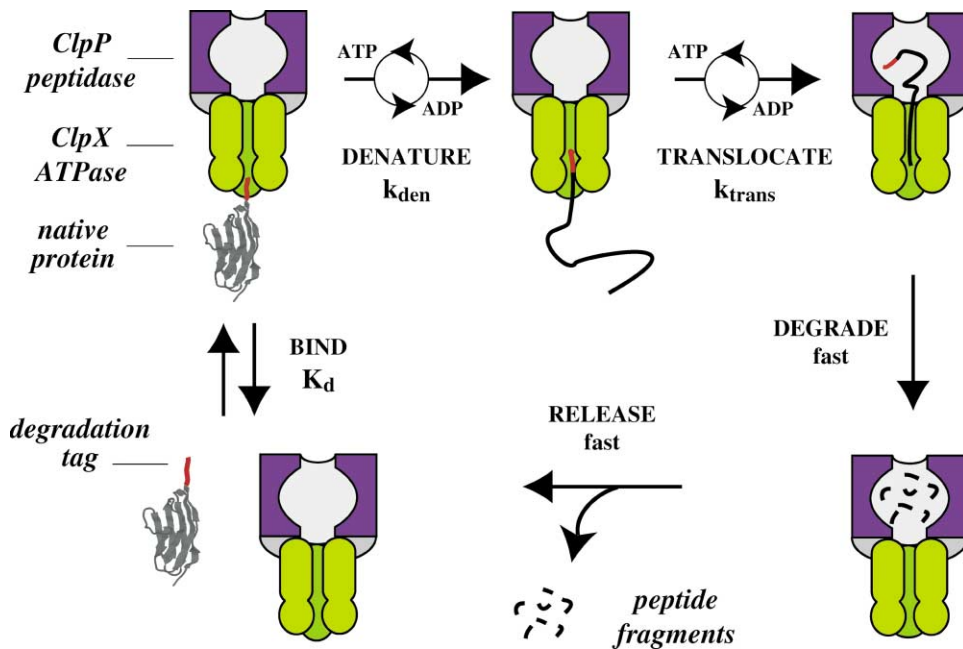


Figure 1. Steps in ATP-Dependent Degradation of Native Protein Substrates by a Compartmentalized AAA⁺ Protease Such as ClpXP
The front half of the ATPase and peptidase complex has been removed to allow a view of the protein processing pore of ClpX and the proteolytic chamber of ClpP. Although degradation and release almost certainly begin to occur before the complete denatured polypeptide has been translocated, for simplicity, the reaction is shown as consisting of discrete translocation, degradation, and release steps.

tagging. As discussed below, an *ssrA*-tagged variant of the I27 domain of titin fulfills each of these criteria.

Here, we show that binding to ClpXP per se does not destabilize titin substrates and that structural elements proximal to the degradation tag of titin resist ClpXP-mediated denaturation. Our studies dissect the denaturation and translocation steps of degradation, show that either step can be rate determining, demonstrate that ATP consumption varies dramatically with the resistance of the substrate to denaturation, and support a model in which denaturation requires numerous repeated applications of a uniform, mechanical unfolding force.

Results

Native and Denatured Titin Variants

To examine ClpXP degradation of a set of native proteins with the same basic structure but different stabilities, we selected the wild-type titin-I27 domain and a group of five mutants with amino acid substitutions (V4A, Y9P, V11P, V13P, and V15P) that alter the equilibrium and/or AFM-induced unfolding of untagged titin (Carrion-Vasquez et al., 1999; Marszalek et al., 1999; Li et al., 2000; Fowler and Clarke, 2001; Fowler et al., 2002). This domain has a simple immunoglobulin fold (Figure 2A) with a buried tryptophan that provides a convenient fluorescent readout of folding status. To permit ClpXP degradation, the *ssrA* tag was appended to the C terminus of each titin variant. Four of the five titin mutants contained disruptions in the β sheet between the A' strand and the G strand to which the *ssrA* tag was appended (Figure 2A), allowing the importance of the

stability of the structural element attached to the degradation tag to be assessed. Equilibrium and kinetic stabilities to GuHCl denaturation were determined for each titin-I27-*ssrA* variant, demonstrating that these proteins display significantly different stabilities in solution. The wild-type *ssrA*-tagged protein was the most stable, V13P was the least stable variant, and the remaining mutants had intermediate stabilities (Table 1; Figure 2B and 2C).

To obtain a molecular mimic for the denatured state of titin-I27-*ssrA*, we used iodoacetic acid to carboxymethylate two cysteines, which are normally buried in the hydrophobic core. Several observations showed that this chemically modified protein was, in fact, denatured: (1) carboxymethyl (CM) titin-I27-*ssrA* had a circular-dichroism (CD) spectrum expected for a random coil (Figure 2D); (2) the fluorescence spectrum of its tryptophan, which is buried and blue-shifted in native titin, was red-shifted to a solvent exposed position in CM-titin-I27-*ssrA* (Figure 2E); and (3) CM-titin-I27-*ssrA* showed no denaturation transition in GuHCl (Figure 2B) or thermal melts (data not shown). Carboxymethylated derivatives of the mutant titin proteins were also prepared and found to be denatured and highly soluble, as was titin-I27-*ssrA* with cysteines modified by reaction with N-ethylmaleimide.

Degradation of Titin Variants by ClpXP

Does the native structure of *ssrA*-tagged titin-I27 slow proteolysis by ClpXP? Measuring the release of acid-soluble peptides from ³⁵S-labeled proteins, we found that ClpXP degraded denatured CM-titin-I27-*ssrA* much faster than native titin-I27-*ssrA* (Figure 3A). Hence, the

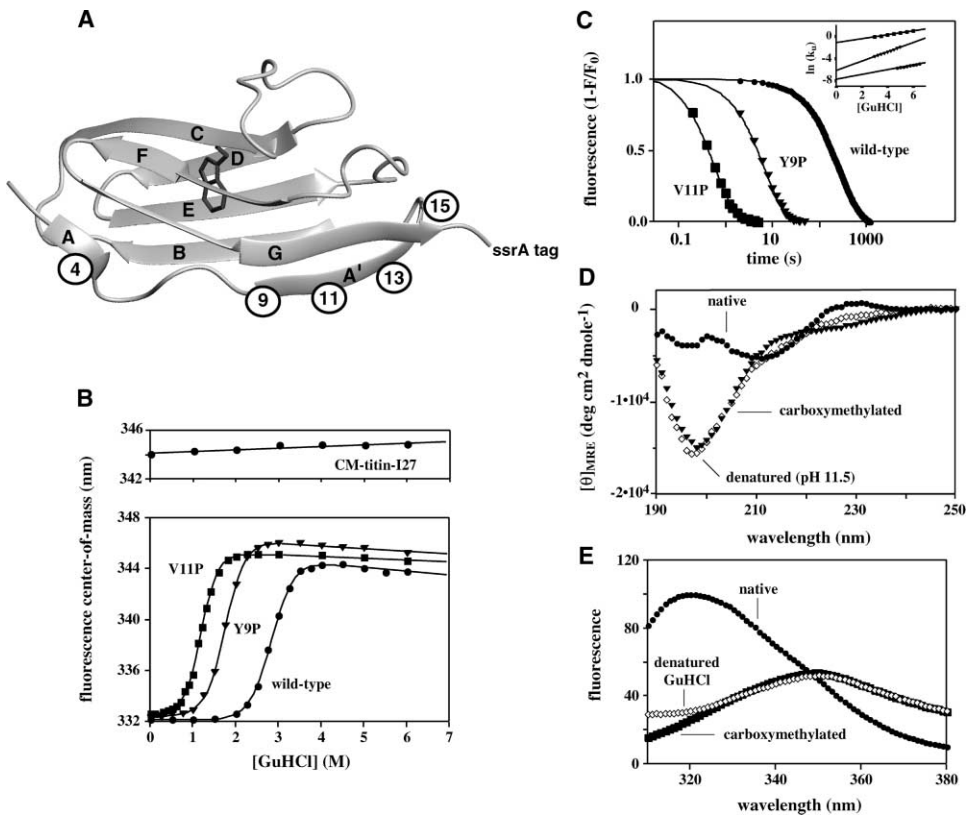


Figure 2. Folding and Stability of Titin-I27-ssrA and Variants

(A) Ribbon model of the secondary structure of the titin-I27 domain (Improta et al., 1996; PDB code 1TIT). The positions of single-substitution mutations, the C-terminal ssrA tag, and the sole tryptophan are shown.
 (B) GuHCl-induced equilibrium denaturation of titin-I27-ssrA and two stability variants assayed by changes in tryptophan fluorescence center-of-mass. The CM-titin-I27-ssrA molecule showed no unfolding transition (upper image).
 (C) Kinetics of unfolding following a jump to 5 M GuHCl for titin-I27-ssrA and two stability variants. Rate constants for these experiments and others performed at different denaturant concentrations are plotted as a function of denaturant in the inset. Equilibrium and kinetic stability parameters derived for native titin-I27-ssrA and its variants are listed in Table 1.
 (D) Denatured titin-I27-ssrA [pH 11.5] and CM-titin-I27-ssrA [pH 7.5] have random-coil far-UV CD spectra very different from that of native titin-I27-ssrA [pH 7.5].
 (E) The fluorescence-emission spectra of titin-I27-ssrA denatured in 5 M GuHCl and CM-titin-I27-ssrA are red-shifted to positions expected for complete solvent exposure of the single tryptophan side chain, which is buried in the native protein.

folded structure of titin-I27 impedes degradation, suggesting that denaturation is rate limiting for ClpXP proteolysis of this molecule. However, the V13P mutant was degraded at a rate close to that of fully denatured titin (Figure 3A). Although this mutant is less stable than wild-type, it is sufficiently stable so that 99% or more of the ensemble of molecules are still folded in solution. As a result, both the structure and stability of native titin appear to play roles in determining the degradation rate by ClpXP.

How do the distinct structural stabilities of the ssrA-tagged titin-I27 variants affect their binding to and rates of proteolysis by ClpXP? To address these questions, steady-state degradation rates were determined over a range of substrate concentrations for each titin-I27-ssrA variant both in unmodified and carboxymethylated forms. In each instance, the observed degradation rates displayed Michaelis-Menten saturation kinetics (Figure 3B). Values of the rate constant for the overall degradation reaction (k_{deg}) varied from 0.25 min^{-1} to 4.9 min^{-1} (Table 2) and were highest for the least stable native

proteins and the carboxymethyl derivatives. Hence, destabilizing native titin causes a general increase in ClpXP degradation rates. For the denatured substrates, changes in sequence or the type of cysteine modification did cause some differences in ClpXP degradation rates (Table 2) but these were minor compared to differences between native variants. Averaging the rate constants for degradation of the seven denatured titin molecules tested gave a value of $4.3 \pm 0.5 \text{ min}^{-1}$.

ClpXP degradation of the native and denatured titin variants showed similar concentration dependencies (Figure 3B; Table 2), with an average K_M ($1.5 \pm 0.5 \mu\text{M}$) close to values determined for other ssrA-tagged proteins and to the K_D for ClpX binding to an ssrA peptide (Kim et al., 2000; Burton et al., 2001a; Wah et al., 2002). Moreover, K_M and k_{deg} for the set of titin variants were uncorrelated ($R^2 < 0.01$), as expected if K_M is approximately equal to K_D for binding (If K_D , k_d , and k_a are the equilibrium dissociation constant, dissociation rate constant, and association rate constant, respectively, for the interaction of substrate with ClpX, then $K_M = (k_d +$

Table 1. Effect of Mutations on Thermodynamic, Kinetic, and Mechanical Stability of titin I27-ssrA

Variant	ΔG_u^a (kcal mol ⁻¹)	m_{D-N} (kcal mol ⁻¹ M ⁻¹)	$k_u^{H_2O}^b$ (min ⁻¹)	$m_{\pm N}$ (kcal mol ⁻¹ M ⁻¹)	pN ^c
I27-ssrA	6.4	2.3	0.026	0.43	204
V4A-I27-ssrA	4.4	2.5	0.17	0.64	204 ^d
Y9P-I27-ssrA	4.5	2.6	0.13	0.84	266
V11P-I27-ssrA	3.5	3.0	19	0.35	143
V13P-I27-ssrA	2.9	2.7	32	0.19	132
V15P-I27-ssrA	4.6	2.3	2.3	0.16	159

Errors in ΔG_u , k_u , and m -values are estimated to be 5–10%.

^a ΔG_u and m_{D-N} values derived from fits of data like that shown in Figure 2B.

^b Values for $k_u^{H_2O}$ and $m_{\pm N}$ were derived from fits of data like that shown in Figure 2C inset.

^c pN values except for V4A-ssrA were calculated from AFM force extension curves at a pulling speed of 0.6 nm ms⁻¹ as reported in Li et al., 2000.

^d The V4A mutation is reported to have no significant effect on the mechanical stability of the titin module (Fowler et al., 2002). We set the pN value for V4A equal to that for wild-type titin-I27.

$k_{deg}/k_a \approx K_D$ when $k_d \geq k_{deg}$). Thus, ClpXP binds each titin substrate in a comparable fashion. These results show that the interaction of the ssrA-tagged titin variants with ClpXP is determined principally by the ssrA tag and not by the structural properties or stability of the attached protein.

Translocation and the Degradation of Denatured Substrates

Several experiments suggest that translocation is the step in the Figure 1 reaction cycle that limits the rate of

ClpXP degradation of denatured titin-I27 at saturating substrate concentrations. First, we found that an unstructured peptide with an ssrA tag as the last 11 amino acids (18 residues total) was degraded at a rate of 41 ± 5 molecules min⁻¹ per enzyme (Figure 3C), which was much faster than the rate of degradation of denatured titin-I27-ssrA (121 residues) and roughly proportional to its decreased length relative to titin. Thus, steps that should occur at the same rate for both short and long substrates (e.g., tag binding and engagement) are not rate limiting for steady-state degradation of titin sub-

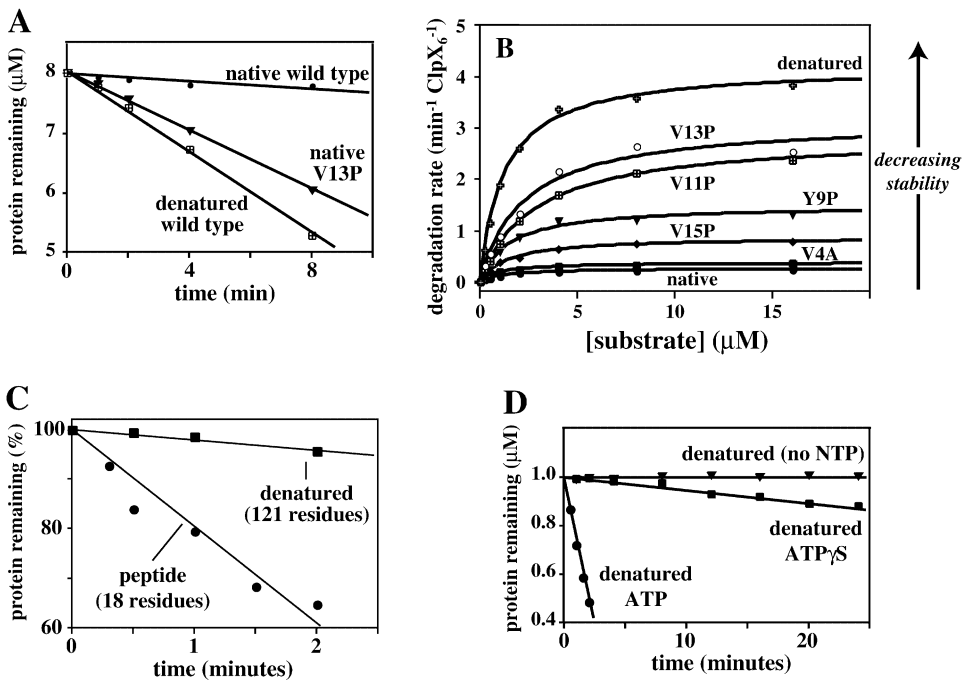


Figure 3. Kinetics of ClpXP Degradation of Titin-I27-ssrA and Variants

(A) Kinetics of ClpXP degradation assayed by release of acid-soluble radioactivity from ³⁵S-labeled titin-I27-ssrA (8 μ M), the native V13P mutant (8 μ M), or denatured CM-titin-I27-ssrA (8 μ M). Degradation required ATP, ClpX, ClpP, and the ssrA-tagged form of titin-I27 (not shown).

(B) Michaelis-Menten plots of the dependence of ClpXP degradation rates on the concentration of the titin-I27-ssrA or variant substrates. The “denatured” curve represents average values for CM-titin-I27-ssrA and the three carboxymethylated mutant variants. Fitted values for k_{deg} ($V_{max}/[ClpX_6]$) and K_M are listed in Table 2.

(C) Degradation of a synthetic 18-residue peptide NH₂-NKKGRHGAANDENYALAA-COOH (20 μ M) by ClpXP.

(D) Relative to ATP, ATP- γ S supports slow ClpXP degradation of denatured CM-titin-I27-ssrA (1 μ M). ClpXP hydrolyzes ATP- γ S approximately 25-fold more slowly than ATP (Burton et al., 2003). In all images, the ClpXP concentration was 0.1 μ M in terms of the ClpX hexamer.

Table 2. Effect of Mutations on the Steady State Kinetic Parameters for ClpXP Degradation of titin-I27-ssrA

I27-ssrA Variant	ClpXP, k_{deg}^a $\text{min}^{-1} [\text{ClpXP}]_e^{-1}$	ClpXP, K_M (μM)	k_{den}^b (min^{-1})	ATPase rate ^c $\text{min}^{-1} [\text{ClpXP}]_e^{-1}$	ATP per titin degraded ^d
wild-type	0.25	1.4	0.27	161	644
V4A	0.36	1.1	0.39	168	467
Y9P	1.5	1.6	2.3	217	145
V11P	2.9	2.9	8.9	356	123
V13P	3.1	2.3	11	366	118
V15P	0.85	1.5	1.1	200	235
CM wild-type	3.7	1.0	-	609	165
CM V4A	4.3	1.1	-	ND	ND
CM Y9P	4.5	1.6	-	ND	ND
CM V11P	4.3	1.3	-	605	141
CM V13P	4.9	1.3	-	582	119
CM V15P	3.7	1.4	-	639	173
NEM wild-type	4.6	1.5	-	ND	ND

Errors in k_{deg} and K_M were estimated to be $\pm 10\%$ based on replicate measurements. Errors in ATPase rates were $\pm 7\%$.

^a K_M and k_{deg} values for ClpXP degradation are from nonlinear least squares fits of data like that shown in Figure 3B.

^b k_{den} values calculated as $(k_{trans} * k_{deg}) / (k_{trans} - k_{deg})$ based on Figure 1 model, assuming denaturation and/or translocation is rate-limiting.

^c With 20 μM protein substrate and 2.5 mM ATP.

^d ATPase rate/ k_{deg} .

strates. The time required to translocate an entire substrate molecule, however, should depend on its length, whereas peptide-bond hydrolysis and product release, which could also depend on length, are too fast to be rate limiting (Thompson and Maurizi, 1994; Thompson et al., 1994).

Both protein denaturation and translocation by ClpXP require ATP-hydrolysis (Singh et al., 2000; Burton et al., 2003). Thus, degradation of denatured titin by ClpXP should be ATP-dependent if translocation is the slow step in its proteolysis. In fact, denatured CM-titin-I27-ssrA was not degraded when ATP was omitted from the reaction and was degraded much more slowly in the presence of ATP γ S (Figure 3D), which is also hydrolyzed by ClpXP but at a much slower rate than ATP (Burton et al., 2003). We conclude that translocation is rate-limiting for degradation of denatured titin substrates and assign this step a rate constant (k_{trans}) equal to the average rate constant for denatured titin degradation ($4.3 \pm 0.5 \text{ min}^{-1}$).

Denaturation and translocation both contribute to the observed degradation rates of some native titin variants. Using the average value of k_{trans} and assuming that denaturation and/or translocation are the slow steps permits the denaturation rate constant (k_{den}) for ClpXP unfolding of different titin variants to be calculated (Table 2). Specifically, because the average time required for degradation ($\tau_{deg} = 1/k_{deg}$) is just the average time for denaturation plus translocation ($\tau_{den} + \tau_{trans}$), then $1/k_{den} = 1/k_{deg} - 1/k_{trans}$.

ATP Consumption during Titin Processing

How efficiently does ClpXP use ATP hydrolysis to drive the substrate denaturation and translocation steps required for degradation of different titin-I27 variants? To address this question, the relationship between the ATPase and protein processing activities of ClpXP was assessed by measuring ATP hydrolysis rates at substrate concentrations where most enzyme molecules ($\sim 90\%$) were actively engaged in degradation (Figure

4A). ATP turnover was fast during degradation of denatured titin variants ($609 \pm 43 \text{ min}^{-1}$). We take this value as the ATPase rate during substrate translocation. For the native titin variants, ATPase activity slowed markedly during degradation and was well correlated with the resistance of these substrates to degradation (Figure 4A). Slowing of the ATPase activity also occurs when ClpXP degrades more stable Arc-ssrA substrates and has been interpreted as evidence for coupling between the ATPase and denaturation cycles (Burton et al., 2001a).

For native titin substrates, both the denaturation and translocation steps of the degradation reaction contribute to ATP hydrolysis, and ATP consumption is thus a function both of the ATP hydrolysis rates during the individual denaturation and translocation steps and of the average time required to complete each of these steps.

$$\text{ATP consumed} = \text{ATP-rate}^{\text{overall}} \bullet \tau_{\text{deg}} = \text{ATP-rate}^{\text{den}} \bullet \tau_{\text{den}} + \text{ATP-rate}^{\text{trans}} \bullet \tau_{\text{trans}}$$

Strikingly, ATP consumption during ClpXP degradation of the native variants varied linearly with τ_{den} with a slope of $144 \pm 3 \text{ min}^{-1}$ and an intercept of 100 ± 6 ($R^2 = 0.998$; Figure 4B). Thus, the average ATP hydrolysis rate during denaturation of native titin variants is constant and roughly 4-fold slower than the ATPase rate during translocation.

These results suggest that, during titin processing, the ATPase motor of ClpXP operates at two basic speeds: fast ($\approx 600 \text{ min}^{-1}$) during translocation of unfolded titin and slow ($\approx 150 \text{ min}^{-1}$) during denaturation of native titin. Because the ATP hydrolysis rate was constant during denaturation of different native variants, irrespective of their intrinsic stabilities, the ease or difficulty of titin unfolding does not affect ClpXP motor speed. Hence, the ATPase and denaturation activities of ClpXP appear to be coupled only loosely. This could occur if the native protein substrate slips or dissociates

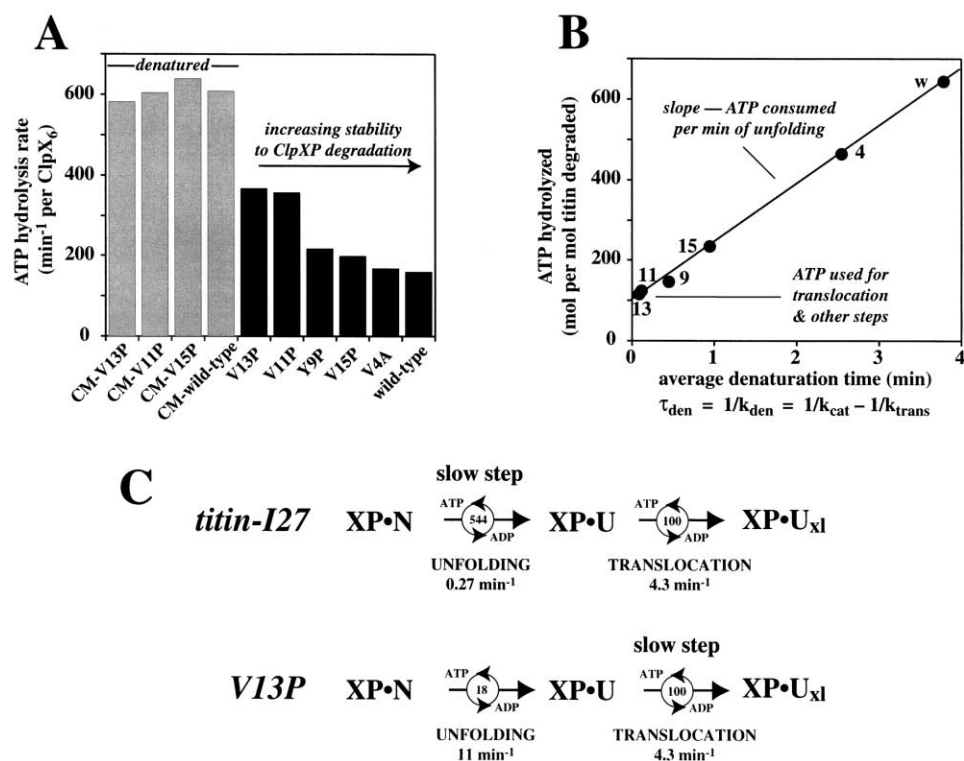


Figure 4. ATP Hydrolysis during ClpXP Degradation of Titin-I27-ssrA Variants

(A) Initial rates of hydrolysis of ATP (2.5 mM) by ClpXP assayed in the presence of native or denatured titin-I27-ssrA variants (20 μ M). The native variants are arranged in order of increasing stability to degradation by ClpXP.

(B) Total ATP consumption during degradation of native titin-I27-ssrA variants ($\text{ATPase rate} \cdot \tau_{\text{den}}$) increases linearly with the average denaturation time ($\tau_{\text{den}} = 1/k_{\text{den}}$). The solid line represents the equation $\text{ATP} = 144 \cdot \tau_{\text{den}} + 100$ ($R^2 = 0.998$).

(C) ATP expenditure during ClpXP degradation of one molecule of wild-type titin-I27-ssrA or the native V13P variant is shown in the circles for the denaturation and translocation steps. Denaturation is the slow or rate-determining step for degradation of wild-type titin-I27. Translocation is the slow step for degradation of the V13P mutant.

transiently when unfolding does not occur during a single cycle of ATP hydrolysis and conformational change within ClpXP. In this regard, slipping of the degradation tag relative to its ClpXP binding site would serve as a “clutch” permitting the ATPase motor to disengage rather than stall.

The intercept of the Figure 4B plot (100 ± 6 ATP per titin degraded) represents the average energetic cost of translocation and any remaining ATP-dependent steps other than denaturation. We assume that most of this ATP is consumed during translocation. For the denatured CM-titin molecules, the average total cost of degradation was slightly higher (149 ± 25 ATP molecules per titin degraded). This small difference may reflect experimental error or a higher translocation cost for carboxymethylated proteins.

Although ATP hydrolysis was fastest when ClpXP degraded unfolded substrates (Figure 4A), ATP consumption was much higher for degradation of stable native substrates (Figure 4B). To denature and degrade more stable protein substrates, ClpXP simply uses more ATP. For wild-type titin-I27-ssrA, $\sim 84\%$ of the ATP consumed during degradation (544 of 644 molecules) was used for denaturation (Figure 4C). The need for so many cycles of ATP hydrolysis to denature a single titin-I27-ssrA molecule suggests strongly that unfolding is a stochastic process that requires a repeated or iterative application

of force. By contrast, for degradation of the V13P variant, only about 15% of the ATP (18 of 118 molecules) was used for denaturation (Figure 4C). Thus, stabilizing the β sheet attached to the ssrA-tag of wild-type titin-I27 relative to the V13P mutant increased the number of ATP cycles required for ClpXP-catalyzed denaturation almost 30-fold.

Discussion

The studies presented here have allowed us to dissect the rates and ATP requirements for the denaturation and translocation steps during ClpXP degradation of a set of titin-I27-ssrA substrates. These results, in turn, improve our understanding of ClpXP function and permit comparisons with other substrates and AAA⁺ proteases. In the discussion below, we first address the question of the relationship of protein stability to denaturation and degradation rates by ClpXP. We then return to the issue of ATP utilization and comparisons with other systems.

Role of Local Versus Global Substrate Stability in Resisting ClpXP Unfolding

For titin-I27-ssrA and its variants, the rate constants for ClpXP denaturation showed reasonable correlations with thermodynamic stability, kinetic stability, and the

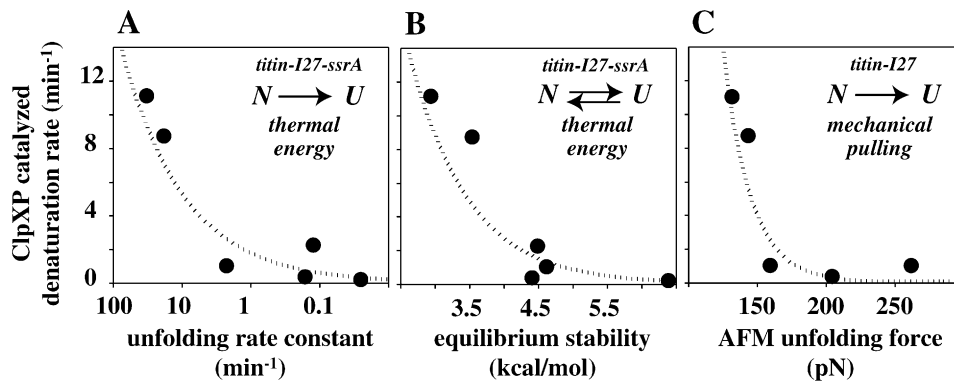


Figure 5. Denaturation Rates and Stability

ClpXP denaturation rates for the titin-I27-ssrA variants correlate with (A) kinetic stability; (B) equilibrium stability (ΔG_u); and (C) mechanical stability in AFM experiments for the untagged molecules (Li et al., 2000; Fowler and Clarke, 2001; Fowler et al., 2002). The dotted lines are exponential or power fits but have no theoretical basis.

force required for AFM-induced unfolding (Figure 5). In principle, these correlations could be interpreted in terms of changes in local or global protein stability. However, global thermodynamic or kinetic stability does not appear to be an important factor when these properties are compared with ClpXP degradation rates for different protein families. For example, the rates of ClpXP degradation of 13 different ssrA-tagged native substrates (GFP-ssrA; Kim et al., 2000); RNase-H⁺-ssrA (our unpublished data); 5 Arc-ssrA variants (Burton et al., 2001a); and 6 titin-I27-ssrA variants) showed no significant correlation ($R^2 < 0.05$) with either the free energy of unfolding or the unfolding rate constant (Figure 6). Individual comparisons emphasize the lack of correlation. One Arc-ssrA substrate, for example, unfolds roughly 6500-fold more slowly than titin-I27-ssrA but was degraded 5-fold more rapidly (Burton et al., 2001a). Similarly, RNase H⁺-ssrA is 6 kcal/mol more thermodynamically stable than titin-I27-ssrA but was degraded 20-fold more rapidly than native titin and as fast as denatured titin. Although differences in translocation rates may also contribute to some of these poor correlations, it seems highly unlikely that global substrate sta-

bility is a critical factor in determining ClpXP degradation rates.

The local stability model of Matouschek and colleagues (Lee et al., 2001; Matouschek, 2003) ascribes the differences observed in ClpXP-mediated degradation of the titin variants to changes in the stability of the structural element attached to the C-terminal ssrA tag. Specifically, interactions between the titin A' and G β strands, which were disrupted by four of the five titin mutations studied here, would represent the principal energy barrier to ClpXP-mediated unfolding. This β sheet of titin displays striking mechanical stability in AFM stretching experiments and in molecular-dynamics simulations (Liu et al., 1998; Marszalek et al., 1999; Li et al., 2000). Hence, it is reasonable that destabilization of this structure would allow easier denaturation and thus faster ClpXP degradation. The local stability model explains our finding that titin mutations (Y9P, V11P, V13P, and V15P), which disrupt the ssrA-proximal β sheet, increased the ClpXP degradation rate far more than a mutation (V4A), which alters a side chain distant from the ssrA tag. Because denaturation of single-domain proteins is generally highly cooperative, ClpXP

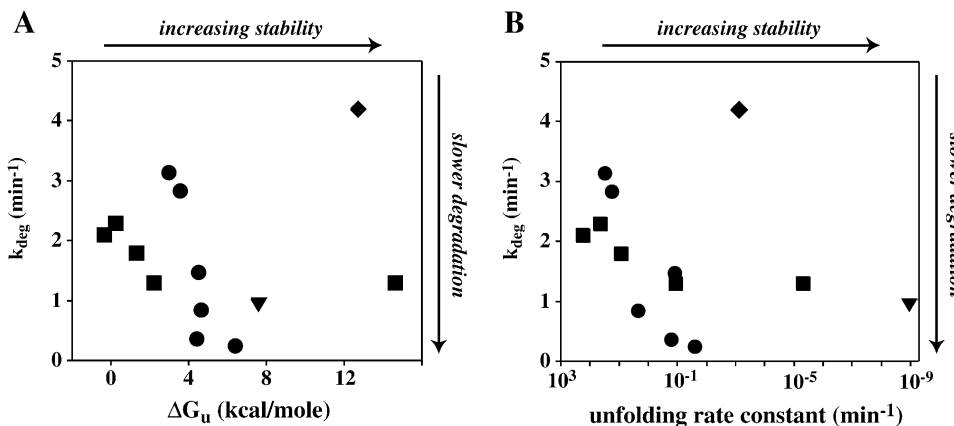


Figure 6. Relationship between Degradation and Stability for ssrA-Tagged Substrates from Different Protein Families

ClpXP degradation rates do not correlate well with the equilibrium stability (A) or kinetic stability (B) for nonrelated proteins. In both images, titin-I27-ssrA variants are shown as circles, Arc-ssrA variants are shown as squares, GFP-ssrA is a triangle, and RNase-H⁺-ssrA is a diamond.

unfolding of structural elements adjacent to the degradation tag should result in global unfolding. Indeed, because titin-I27-ssrA is degraded by ClpXP in spite of its extraordinary C-terminal stability, we suspect that very few single-domain ssrA-tagged proteins will be refractory to ClpXP denaturation and thus degradation.

If force is mainly applied through the degradation tags of protein substrates by ClpXP and related AAA⁺ enzymes, then it becomes crucial whether this tag is attached to a relatively stable or fragile region of the protein structure (Lee et al., 2001; Matouschek, 2003). Hydrogen-exchange studies monitored by NMR show that different regions of a protein can have dramatically different local stabilities (Bai et al., 1995; Chamberlain et al., 1996). Substrates like GFP-ssrA and RNase-H*-ssrA, which are more globally stable than titin-ssrA but are degraded faster by ClpXP (Figure 6), would therefore be expected to have relatively fragile structures at their C termini. Indeed, native-state hydrogen-exchange studies show that the C-terminal α -helix of RNase-H* is the least stable structural element in this protein (Hollien and Marqusee, 1999).

Mechanical Denaturation

AFM denatures proteins by mechanical deformation, making it of interest to compare this process with that suggested for ClpXP-mediated denaturation. By stretching a protein molecule from two different points, AFM increases the applied force continuously until denaturation occurs. ClpXP, by contrast, appears to apply force iteratively in a series of pulling and slipping reactions involving the degradation tag. Opposing “unfolding” and “slip” forces presumably arise when ATP-dependent conformational changes in ClpXP attempt to pull native proteins, which resist denaturation, into a pore too small to allow transit without denaturation. By this model, the same ClpXP conformational changes that drive substrate translocation would also drive substrate denaturation.

Although the AFM and ClpXP mechanisms of unfolding seem to be fundamentally different, it is nevertheless instructive to consider issues of force. To achieve a rate of wild-type titin-I27 denaturation equivalent to that accomplished by ClpXP, an AFM mechanism would require a force of 43 pN. This value was calculated as $\text{force} = (kT/\Delta x) \cdot \ln(k_{\text{den}}/\alpha_0)$, where k is the Boltzmann constant, T is the temperature, Δx is the titin transition-state distance, k_{den} is the rate constant for ClpXP-mediated titin denaturation, and α_0 is the rate constant for titin unfolding at zero force (Li et al., 2000; Carrion-Vasquez et al., 2003). If ClpX acts in an iterative fashion, however, then the overall force that it applies to titin during each mechanical event would need to be greater than the AFM force. This possibility appears plausible, as an AAA⁺ ATPase has been shown to generate forces of 100 pN or more (Maier et al., 2002).

Although it seems clear that ClpXP-mediated unfolding of protein substrates is mechanically driven, it is formally possible that substrate binding to the enzyme places it in an electrostatic or hydrophobic environment that contributes to the overall process by making denaturation easier. However, if native titin-I27-ssrA were significantly less stable when bound to ClpXP than in

solution, then thermodynamic linkage would require that denatured titin-I27-ssrA bind the enzyme with significantly higher affinity. This result was not observed. As a result, we conclude that binding to ClpXP is not a major factor in titin destabilization or denaturation.

ATP Utilization during Different Steps of ClpXP Degradation

Our ability to study ClpXP degradation of titin-I27-ssrA substrates in native and denatured forms has demonstrated that either denaturation and/or translocation can be rate limiting depending on the physical state and stability of the titin substrate. Moreover, knowing the average times required for each step for specific substrates allows the ATP utilization during each reaction to be determined. One of our most striking results was that denaturation of a single native titin molecule consumed a highly variable amount of ATP depending on the stability of the titin variant and the time required for denaturation. As shown in Figure 4C, ClpXP denaturation of wild-type titin-I27 required more than 500 cycles of ATP hydrolysis, whereas denaturation of the native V13P variant, which has a less stable C-terminal β sheet, required fewer than 20 ATP cycles. Clearly, ClpXP simply uses more cycles of ATP hydrolysis when confronted with substrates, like wild-type titin-I27, that are difficult to unfold. This gives rise to a highly robust unfolding activity that is almost certainly important for the ability of ClpX, in the absence of ClpP, to disassemble hyperstable macromolecular complexes (Burton et al., 2001b).

It is worth emphasizing the relationship between the average number of ClpXP enzymatic cycles required to denature a given substrate and the probability of denaturation during a single cycle. If ClpXP denaturation is a stochastic process, as we have argued, then a given substrate will have a fixed probability of denaturation during each enzyme cycle. For substrates with highly stable C termini, like titin-I27-ssrA, this probability is low and thus many ATP cycles are needed before most of the molecules in the population become denatured. For molecules with less stable C termini, like the V13P variant, this unit unfolding probability is high and thus only a relatively small number of enzyme turnovers are required to denature most substrate molecules.

Protein degradation by ClpXP can clearly be very costly, especially when protein substrates are hard to denature. For comparison, we note that ClpXP uses more energy to degrade one molecule of wild-type titin-I27-ssrA than is required for the biosynthesis of this protein. Indeed, degradation is expensive even when the target protein is already denatured. Degradation of unfolded forms of the 121-residue titin-I27 substrates consumed 100–150 molecules of ATP. If, as seems probable, most of this ATP is used for translocation, then the average cost of ClpXP translocation for titin-I27 is close to one ATP per amino acid. It will be interesting to determine how the rate and energetic cost of translocation vary with the sequence and length of the protein substrate.

Slipping and Substrate Release

The ATPase motor of ClpXP was found to operate at a constant hydrolysis rate during denaturation of titin

substrates with very different stabilities. We have interpreted this result as evidence that application of a denaturing force during each ATP cycle must be interrupted by disengagement or slipping of the protein substrate from the grasp of ClpXP when denaturation fails. In a practical sense, the ability to release a substrate that cannot be denatured in a single enzymatic cycle would prevent the ClpXP machine from becoming jammed. This feature is probably important both for substrates that are simply too stable to be unfolded and for substrates, like wild-type titin-ssrA, that require a large number of ATP hydrolysis events to achieve efficient denaturation.

If substrates can slip or disengage from ClpXP, then it also seems likely that the slip force will depend on the amino acid sequence of the degradation tag or the sequence being translocated when a native protein domain is encountered. At present, however, almost nothing is known about the relationship between sequence and slippage. Performing assays of ATP utilization, like those shown in Figure 4B, for titin variants with different types of C-terminal degradation tags should allow this question to be addressed.

Comparisons with Other Substrates and AAA⁺ Enzymes

In a prior study, ClpXP was found to degrade Arc-ssrA substrates that varied dramatically in global stability with only modest changes in degradation rates (Burton et al., 2001a). As in the titin-I27 studies, however, more stable Arc-ssrA variant were degraded more slowly by ClpXP. Because the Arc-ssrA variants had stability mutations located far from the ssrA tag, it seems likely that the local stability near the ssrA tag was not affected significantly by these mutations. ClpXP degradation of the Arc-ssrA substrates also consumed a relatively constant amount of ATP per Arc molecule degraded (150 ± 20). Based on the results presented here, we suspect that translocation of the Arc substrates consumed most of this ATP. Unfortunately, fully denatured variants of Arc were not available and thus the energetic cost of denaturation and translocation could not be determined. In another study, native and acid-denatured GFP-ssrA appeared to be degraded at similar rates and a cost of 300–400 ATPs by the PAN/20S protease (Benaroudj et al., 2003). Again, it is possible that translocation represents the major ATP cost for this substrate, although refolding of acid-denatured GFP-ssrA occurs readily and could complicate interpretation of these experiments.

Although some discrepancies between different substrates and/or enzymes might represent real differences in mechanism, it is more likely that the substrates chosen to probe mechanism are critical in determining the results obtained. For example, had we simply assayed ClpXP degradation of the V11P and V13P titin-I27-ssrA proteins in native and denatured forms, we would have observed that roughly the same amount of ATP was required for degradation and that the native structure of these proteins imposed only a minor impediment to degradation. While clearly true for these particular substrates, this conclusion is highly misleading for ClpXP degradation of other titin substrates and obscures the

underlying mechanism. Our results suggest that a full understanding of mechanism for any particular AAA⁺ protease will require analyses of a set of substrates with a range of local protein stabilities near the degradation tag and the ability to study degradation of these substrates in native and fully denatured forms. In this regard, we anticipate that titin-I27 substrates with appropriate degradation tags should help in dissection of reaction mechanisms for other AAA⁺ degradation and disassembly machines and also permit more detailed studies of the ClpXP translocation and denaturation reactions.

Experimental Procedures

Protein Production

Genes expressing titin-I27-ssrA or variants were constructed by PCR from the I27 domain of human titin subcloned in pET Ava I (Carrion-Vasquez et al., 1999). The N-terminal sequence of each construct was MH₆S₂HID₄KLGLIEVE and the C-terminal sequence was **KVKELGLGAANDENYALAA** (titin-I27 sequences bold italic; ssrA tag underlined). Proteins were expressed in *E. coli* strain JK10 (*clpP::cat*, Δlon , *slyD::kan*, λ DE3) with an appropriate plasmid, purified by Ni²⁺-NTA chromatography, and masses confirmed by MALDI-TOF mass spectrometry. ³⁵S proteins were expressed as described (Gottesman et al., 1998) and purified like unlabeled protein. CM-cysteine derivatives of the I27-ssrA variants were obtained by alkylation for 2 hr (25°C) with a 100-fold molar excess of iodoacetic acid in the presence of 5 M GuHCl at pH 8.8. Mass spectrometry verified the presence of two carboxymethyl groups per titin-I27-ssrA molecule. CD experiments were performed using an AVIV 60DS spectrometer with 10 μ M protein samples in 10 mM phosphate buffer [pH 7.5] or in 2.8 mM KOH [pH 11.5].

Equilibrium Denaturation and Unfolding Kinetics

Purified titin-I27-ssrA or variants (1 μ M) were mixed with different concentrations of GuHCl plus buffer A (50 mM Tris•HCl [pH 7.5], 150 mM NaCl, 2 mM DTT). Following equilibration at 30°C, fluorescence emission spectra were recorded. Plots of denaturant concentration versus fluorescence center-of-mass were fitted to obtain values of ΔG_{D-N} , m_{D-N} , and the slopes and intercepts of the native and denatured baselines (Santoro and Bolen, 1998). Unfolding rates at 30°C were determined at different concentrations of GuHCl in buffer A. For titin-I27-ssrA and the Y9P and V15P variants, proteins were diluted by manual mixing from native conditions into GuHCl (1 μ M final protein concentration) and decreases in fluorescence emission at 340 nm (excitation 280 nm) were monitored. For the V11P and V13P variants, unfolding was monitored using a stopped-flow instrument at final protein concentrations of 16–20 μ M. Kinetic trajectories at each GuHCl concentration fit well ($R^2 > 0.98$) to a single exponential function.

Degradation and ATPase Assays

Degradation of titin-I27-ssrA or variants by ClpXP was performed at 30°C in 25 mM HEPES [pH 7.6], 100 mM KCl, 10 mM MgCl₂, 10% glycerol, and 2 mM DTT with an ATP regeneration system (5 mM ATP, 16 mM creatine phosphate, and 0.032 mg/mL creatine kinase). ClpX₆ and ClpP₁₄ were a gift from R. Burton (MIT) and were used at concentrations of 100 and 300 nM, respectively. ClpXP was preincubated for 2 min at 30°C with all assay components except substrate protein. Reactions were performed in a volume of 100 μ l and initial degradation rates for wild-type titin-I27-ssrA were determined by release of TCA-soluble peptides (Gottesman et al., 1998). ATPase assays were performed as described (Norby, 1988; Burton et al., 2001a). For peptide degradation, cleavage was assayed by HPLC.

Acknowledgments

Supported by NIH grant AI-15706. We thank Steve Bell, Randy Burton, Mariano Carrion-Vasquez, Hongbin Li, Susan Marqusee, Frank Solomon, and members of the Baker and Sauer labs for materials, advice, and helpful discussions.

Received: April 15, 2003
Revised: June 24, 2003
Accepted: July 21, 2003
Published: August 21, 2003

References

- Bai, Y., Sosnick, T.R., Mayne, L., and Englander, S.W. (1995). Protein folding intermediates: native-state hydrogen exchange. *Science* 269, 192–197.
- Benaroudj, N., Zwickl, P., Seemuller, E., Baumeister, W., and Goldberg, A.L. (2003). ATP hydrolysis by the proteasome regulatory complex PAN serves multiple functions in protein degradation. *Mol. Cell* 11, 69–78.
- Burton, R.E., Siddiqui, S.M., Kim, Y.I., Baker, T.A., and Sauer, R.T. (2001a). Effects of protein stability and structure on substrate processing by the ClpXP unfolding and degradation machine. *EMBO J.* 20, 3092–3100.
- Burton, B.M., Williams, T.L., and Baker, T.A. (2001b). ClpX-mediated remodeling of mu transposasomes: selective unfolding of subunits destabilizes the entire complex. *Mol. Cell* 8, 449–454.
- Burton, R.E., Baker, T.A., and Sauer, R.T. (2003). Energy-dependent degradation: linkage between ClpX-catalyzed nucleotide hydrolysis and protein-substrate processing. *Protein Sci.* 12, 893–902.
- Carrion-Vasquez, M., Oberhauser, A.F., Fowler, S.B., Marszalek, P.E., Broedel, S.E., Clarke, J., and Fernandez, J.M. (1999). Mechanical and chemical unfolding of a single protein: a comparison. *Proc. Natl. Acad. Sci. USA* 96, 3694–3699.
- Carrion-Vasquez, M., Li, H., Lu, H., Marszalek, P.E., Oberhauser, A.F., and Fernandez, J.M. (2003). The mechanical stability of ubiquitin is linkage dependent. *Nat. Struct. Biol.*, in press.
- Chamberlain, A.K., Handel, T.M., and Marqusee, S. (1996). Detection of partially folded molecules in equilibrium with the native conformation of RNaseH. *Nat. Struct. Biol.* 3, 782–787.
- Flynn, J.M., Neher, S.B., Kim, Y.I., Sauer, R.T., and Baker, T.A. (2003). Proteomic discovery of cellular substrates of the ClpXP protease reveals five classes of ClpX-recognition signals. *Mol. Cell* 11, 671–683.
- Fowler, S.B., and Clarke, J. (2001). Mapping the folding pathway of an immunoglobulin domain: structural detail from phi value analysis and movement of the transition state. *Structure* 9, 355–366.
- Fowler, S.B., Best, R.B., Toca Herrera, J.L., Rutherford, T.J., Steward, A., Paci, E., Karplus, M., and Clarke, J. (2002). Mechanical unfolding of a titin Ig domain: structure of unfolding intermediate revealed by combining AFM, molecular dynamics, NMR and protein engineering. *J. Mol. Biol.* 322, 841–849.
- Gonciarz-Swiatek, M., Wawrzynow, A., Um, S.J., Learn, B.A., McMacken, R., Kelley, W.L., Georgopoulos, C., Sliemers, O., and Zylicz, M. (1999). Recognition, targeting, and hydrolysis of the λ O replication protein by the ClpP/ClpX protease. *J. Biol. Chem.* 274, 13999–14005.
- Gottesman, S., Roche, E., Zhou, Y., and Sauer, R.T. (1998). The ClpXP and ClpAP proteases degrade proteins with carboxy-terminal peptide tails added by the SsrA-tagging system. *Genes Dev.* 12, 1338–1347.
- Herman, C., Prakash, S., Lu, C.Z., Matouschek, A., and Gross, C.A. (2003). Lack of a robust unfoldase activity confers a unique level of substrate specificity to the universal AAA protease FtsH. *Mol. Cell* 11, 659–669.
- Hollien, J., and Marqusee, S. (1999). Structural distribution of stability in a thermophilic enzyme. *Proc. Natl. Acad. Sci. USA* 96, 13674–13678.
- Improta, S., Politou, A.S., and Pastore, A. (1996). Immunoglobulin-like modules from titin I-band: extensible components of muscle elasticity. *Structure* 4, 323–337.
- Keiler, K.C., Waller, P.R.H., and Sauer, R.T. (1996). Role of a peptide tagging system in degradation of proteins synthesized from damaged messenger RNA. *Science* 271, 990–993.
- Kim, Y.I., Burton, R.E., Burton, B.M., Sauer, R.T., and Baker, T.A. (2000). Dynamics of substrate denaturation and translocation by the ClpXP degradation machine. *Mol. Cell* 5, 639–648.
- Langer, T. (2000). AAA proteases: cellular machines for degrading membrane proteins. *Trends Biochem. Sci.* 25, 247–251.
- Lee, C., Schwartz, M.P., Prakash, S., Iwakura, M., and Matouschek, A. (2001). ATP-dependent proteases degrade their substrates by processively unraveling them from the degradation signal. *Mol. Cell* 7, 627–637.
- Li, H., Carrion-Vasquez, M., Oberhauser, A.F., Marszalek, P.E., and Fernandez, J.M. (2000). Point mutations alter the mechanical stability of immunoglobulin modules. *Nat. Struct. Biol.* 7, 1117–1120.
- Liu, H., Isralewitz, B., Krammer, A., Vogel, V., and Schulten, K. (1998). Unfolding of titin immunoglobulin domains by steered molecular dynamics simulation. *Biophys. J.* 75, 662–671.
- Maier, B., Potter, L., So, M., Seifert, H.S., and Sheetz, M.P. (2002). Single pilus motor forces exceed 100 pN. *Proc. Natl. Acad. Sci. USA* 99, 16012–16017.
- Marszalek, P.E., Lu, H., Li, H., Carrion-Vasquez, M., Oberhauser, A.F., Schulten, K., and Fernandez, J.M. (1999). Mechanical unfolding intermediates in titin modules. *Nature* 402, 100–103.
- Matouschek, A. (2003). Protein unfolding - an important process in vivo? *Curr. Opin. Struct. Biol.* 13, 98–109.
- Neuwald, A.F., Aravind, L., Spouge, J.L., and Koonin, E.V. (1999). AAA+: a class of chaperone-like ATPases associated with the assembly, operation, and disassembly of protein complexes. *Genome Res.* 9, 27–43.
- Norby, J.G. (1988). Coupled assay of Na⁺,K⁺-ATPase activity. *Methods Enzymol.* 156, 116–119.
- Ogura, T., and Wilkinson, A.J. (2001). AAA+ superfamily ATPases: common structure-diverse function. *Genes Cells* 6, 575–597.
- Ortega, J., Lee, H.S., Maurizi, M.R., and Steven, A.C. (2002). Alternating translocation of protein substrates from both ends of ClpXP protease. *EMBO J.* 21, 4938–4949.
- Santoro, M.M., and Bolen, D.W. (1988). Unfolding free energy changes determined by the linear extrapolation method. 1. Unfolding of phenylmethanesulfonyl-chymotrypsin using different denaturants. *Biochemistry* 27, 8063–8068.
- Singh, S.K., Grimaud, R., Hoskins, J.R., Wickner, S., and Maurizi, M.R. (2000). Unfolding and internalization of proteins by the ATP-dependent proteases ClpXP and ClpAP. *Proc. Natl. Acad. Sci. USA* 97, 8898–8903.
- Thompson, M.W., and Maurizi, M.R. (1994). Activity and specificity of *Escherichia coli* ClpAP protease in cleaving model peptide substrates. *J. Biol. Chem.* 269, 18201–18208.
- Thompson, M.W., Singh, S.K., and Maurizi, M.R. (1994). Processive degradation of proteins by the ATP-dependent Clp protease from *Escherichia coli*. Requirement for the multiple array of active sites in ClpP but not ATP hydrolysis. *J. Biol. Chem.* 269, 18209–18215.
- Vale, R.D. (2000). AAA proteins. Lords of the ring. *J. Cell Biol.* 150, 13–19.
- Wah, D.A., Levchenko, I., Baker, T.A., and Sauer, R.T. (2002). Characterization of a specificity factor for an AAA+ ATPase: assembly of SspB dimers with ssrA-tagged proteins and the ClpX hexamer. *Chem. Biol.* 9, 1237–1245.
- Wang, J., Hartling, J.A., and Flanagan, J.M. (1997). The structure of ClpP at 2.3 Å resolution suggests a model for ATP-dependent proteolysis. *Cell* 91, 447–456.